Article:
Al Khalifa, H, Glover, PWJ and Lorinczi, P (2020) Permeability Prediction and Diagenesis in Tight Carbonates Using Machine Learning Techniques. Marine and Petroleum Geology, 112. 104096. ISSN: 0264-8172

https://doi.org/10.1016/j.marpetgeo.2019.104096

Permeability Prediction and Diagenesis in Tight Carbonates Using Machine Learning Techniques

Al Khalifah, H.*, Glover, P.W.J., Lorinczi, P.**
School of Earth and Environment, University of Leeds, UK
* Email: hussain.khalifah@gmail.com
** Email: p.w.j.glover@leeds.ac.uk, Tel: +44 (0)113 3435213

ABSTRACT. Machine learning techniques have found their way into many problems in geoscience but have not been used significantly in the analysis of tight rocks. We present a case study testing the effectiveness of artificial neural networks and genetic algorithms for the prediction of permeability in tight carbonate rocks. The dataset consists of 130 core plugs from the Portland Formation in southern England, all of which have measurements of Klinkenberg-corrected permeability, helium porosity, characteristic pore throat diameter, and formation resistivity. Permeability has been predicted using genetic algorithms and artificial neural networks, as well as seven conventional 'benchmark' models with which the machine learning techniques have been compared. The genetic algorithm technique has provided a new empirical equation that fits the measured permeability better than any of the seven conventional benchmark models. However, the artificial neural network technique provided the best overall prediction method, quantified by the lowest the root-mean-square error (RMSE) and highest coefficient of determination value (R^2). The lowest RMSE from the conventional permeability equations was from the RGPZ equation, which predicted the test dataset with an RMSE of 0.458, while the highest RMSE came from the Berg equation, with an RMSE of 2.368. By comparison, the RMSE for the genetic algorithm and artificial neural network methods were 0.433 and 0.38, respectively. We attribute the better performance of machine learning techniques over conventional approaches to their enhanced capability to model the connectivity of pore microstructures caused by codependent and competing diagenetic processes. We also provide a qualitative model for the poroperm characteristics of tight carbonate rocks modified by each of eight diagenetic processes. We conclude that, for tight carbonate reservoirs, both machine learning techniques predict permeability more reliably and more accurately than conventional models and may be capable of distinguishing quantitatively between pore microstructures caused by different diagenetic processes.

KEYWORDS: permeability, neural networks, genetic algorithms, machine learning, tight carbonates, MICP, porosity, diagenesis.

Introduction

The permeability of reservoir rocks needs to be measured with a high accuracy in order to maximize the efficiency of hydrocarbon production from unconventional reservoirs (Ma and Holditch, 2015). The pulse-decay method is an efficient method for measuring permeability in very tight rocks (Rashid et al., 2017; Hussein et al., 2017). This technique measures the reduction in the inlet pressure of a fixed volume of gas as it passes into a low permeability sample. However, for very tight core plugs this measurement can take many hours. Furthermore, multiple measurements are required at different gas pressures in order to calculate the Klinkenberg-corrected permeability (Zhang et al., 2013). Since all tight rocks are extremely sensitive to gas slippage, this correction is extremely important if an accurate permeability is required (Akai et al., 2016). Each of these measurements is expensive, and consequently a limited number of core plugs can be measured in any given reservoir. Furthermore, tight carbonate reservoirs have a tendency to be heterogeneous, resulting from patchy development of a range of different diagenetic properties (Al-Zainaldin et al., 2015; Glover et al., 2018), leading to a variability in petrophysical properties and reservoir quality over a range of scales. It is generally not possible to representatively sample and measure the permeability of heterogeneous tight carbonate reservoirs because to do so would require an unfeasibly large and expensive dataset. A quicker, less expensive and more reliable way to estimate the permeability of very tight and heterogeneous reservoir rocks would, therefore, be a valuable and welcome technical resource in the characterisation of these reservoirs.

In this paper, we have assessed the capability of two machine learning techniques for the estimation of the permeability of tight carbonate rocks using a limited set of input parameters that can be obtained easily, cheaply, and often routinely from core analysis measurements. The first technique is the use of artificial neural networks (e.g., Rajasekaran and Pai, 2003), while the second technique uses genetic algorithms (e.g., Cuddy and Glover, 2002; Rajasekaran and Pai, 2003). The results have been compared against the predicted permeabilities from a set of seven of the best currently available theoretical and empirical permeability prediction models (equations) from the literature (e.g., Rashid et al., 2015a; 2015b).

It is not the intention of this paper to be a review of either machine learning, or of neural networks or genetic algorithms, or even a review of the application of these approaches to geophysical problems. There is a very rich literature for the former, the latter is served by a very good reviews (e.g., Van der Baan and Jutten, 2000; Sen and Mallik, 2018). For neural networks alone, there is a distinction to be made between feedforward multilayer perceptron

network (MLPN) and radial basis function (RBF) types. The former, itself has many types, including probabilistic approaches (PNN), time delay neural networks (TDNN), convolutional neural networks (CNN), deep stacking and tensor deep stacking neural networks (DSNN and TDSNN). It is far better that we consider some of the recent applications of machine learning to petrophysical applications. While there are many possible applications, recent advances have included all aspects of petrophysics from logging, through facies determination and rock characterisation to the determination of key parameters for calculating reservoir volumetrics and permeability.

In logging both integrated hybrid neural network (IHNN) (Zhu et al., 2018) and Integrated Deep Learning Models (IDLM) (Zhu et al., 2019a) have been implemented in order to improve the estimation of total organic carbon (TOC) significantly, allowing the characterisation of shale gas reservoirs to be improved, while Onalo et al. (2018; 2019) have used a non-linear autoregressive neural networks with exogenous input (NARX) to estimate the shear and compressional sonic travel times in well logs, finding sufficiently accurate predictions of the actual sonic well logs that many of the sonic properties including sonic porosity, Poisson's ratio were capable of being predicted.

Machine learning has also been used to determine the optimal parameters for reservoir characterisation. A good example of this is Zhu et al.'s recent study (Zhu et al., 2019b) of water saturation in organic shale reservoirs, where the parameters of a shale petrophysical model are calculated using genetic algorithms. The approach does not need electrical measurements as input, which makes it ideally suitable for organic shale reservoirs. The characterisation of fractures in reservoirs is also a multi-parameter problem which cannot be approached simply. A combination of genetic algorithms and back propagation neural networks (BPNN) has been found to have the ability to predict fracture zones using deep and shallow electrical logs as input (Xue et al., 2014).

Facies determination and petrophysical characterisation is a clear beneficiary of machine learning techniques. Back propagation neural networks and convolutional neural networks have been used to improve the estimation of total organic carbon, as well as volatile hydrocarbon and remaining hydrocarbon determinations in shale oil reservoirs (Wang et al, 2019), outperforming conventional methodologies for estimating these parameters.

In this work, we are interested in the prediction of permeability in tight carbonate rocks and the effect of diagenesis. Lim and Kim (2004) proposed fuzzy logic and neural network approaches to the prediction of porosity and permeability in reservoirs, indicating that the approaches showed some potential for future development. Tang (2008) and Tang et al. (2011)

have used probabilistic neural networks to classify facies in carbonate reservoirs with some degree of success. Zhou et al. (2019) have combined the study of diagenesis with the use of a deep-autoencoder random forest algorithm to determine the link between different states of diagenesis and the electrical parameters (*m* and *n* values) of tight gas sandstone reservoirs, while Zhu et al. (2017a; 2017b) were able to produce a reasonable prediction of permeability in tight gas sandstone reservoirs using a complex combination of machine learning techniques and input from NMR data, giving results comparable to those obtained by Rashid et al. (2015b) with conventional permeability prediction approaches.

While there are many papers now available in the literature exploring machine learning methods for permeability prediction, fewer compared approaches together and also with a cohort of conventional prediction methods. In addition, there are very few which concentrate on the prediction of permeability in challenging tight carbonate reservoirs. Considering that this type of unconventional reservoir is likely to be more important in the future, and that conventional experimental determination of permeability in very low permeability rocks is complex, time-consuming and expensive, the use of machine learning could be a method of choice if it is found to be reliable. In this work we also consider the interplay between machine learning efficacy and its derived parameters with the diagenetic processes that control permeability in these rocks.

Dataset

The core plug dataset consisted of 130 samples derived from the Portland Formation, which crops out in quarries on the Isle of Portland in southern England. The samples were all sourced from either the Jordans quarry and mine, or the Fancy Beach quarry, which are all in close proximity at 50°33'10"N 02°26'25"W, and which are operated by Albion Stone. The Isle of Portland is composed mostly of Upper Jurassic marine strata with a small thickness of basal Cretaceous Purbeck Formation on top. The lowest formation to be exposed in the area is the Upper Jurassic Kimmeridge Clay, which occurs beneath Portland Harbour and Castletown and is exposed under the foot of the high northern cliffs. Above it lies the Portland Sand, which is composed largely of marls with some sandy horizons. The true Portland Stone lies above the Portland Sand and consists of the Portland Cherty Series overlain by the Portland Freestone. The Portland Freestone is a well-cemented oolitic limestone. Stone from the various beds of the Portland Freestone have historically and contemporaneously been in much demand as fine

building stone (e.g., St. Paul's Cathedral). The Purbeck sequence lies on top of the Portland Freestone and marks the bottom of the Cretaceous.

The samples used in this work have been sourced from the Base Bed and the Whitbed, which occur in the Portland Freestone, and which are dominated by sparite-cemented oolites (Barton et al., 2011). The Whitbed contains common shells, usually distributed evenly but sometimes concentrated in zones. These shells are commonly cemented. The Base bed is less shelly and commonly contains completely cemented shell moulds. The cemented nature of this rock makes it ideal building stone as well as a good, well-studied tight carbonate reservoir analogue.

Helium porosity ϕ, characteristic pore throat size from mercury injection capillary pressure measurements d_{PT}, formation resistivity factor F, and fluid permeability k were measured on each sample at the University of Aberdeen and by oil service companies in the late 1990s. Table 1 gives a summary of these measurements.

The helium porosity was measured on dried 1.5" core plugs using a helium pycnometer that had been built in the laboratory and optimised to allow measurements to be made with an error of better than ±0.001, and provides measurements with approximately five times better accuracy than typical standard automated commercial pycnometers. Porosity was also calculated by water saturation and Archimedes bulk volume, but the difficulty in fully saturating these tight carbonates resulted in discrepancies of greater than 0.05, which led us to discount using the saturation porosity measurements for permeability prediction with conventional methods. The mercury injection capillary measurements were made with a Micromeritics Autopore V, with a maximum applied pressure of 60,000 psi. Formation factor was calculated from saturated sample conductivity and saturating fluid resistivity, both measured using a Quadtech LCR meter at the frequency where the quadrature component was minimised (approximately 1 kHz) according to the methodologies set out in Glover (2015). The observed incompleteness of saturation in some samples leads us to believe that the formation factors and cementation exponents measured in this work may be in more error than some of the other core measurements. However, as we will see later, such errors do not translate into large errors in predicted permeability when using conventional permeability prediction equations.

Since it is a critical parameter in the comparative analyses carried out in this work, a considerable amount of effort was put into measuring the permeability of the samples accurately using both steady-state measurements and pulse-decay measurements. The former of these was used to measure the higher permeability samples, while the latter was used for the

tighter samples. Klinkenberg-corrected steady-state helium gas permeability was measured on a bespoke gas permeability rig composing three ranges of gas pressure application and three ranges of gas flow measurement. Pulse-decay measurements were made using helium as the process gas according to the methodology given in Jones (1997). For both the steady-state and pulse-decay measurements, Klinkenberg corrections were made based on at least 5 effective pressure measurements, while measurements which did not provide the required linear plot of apparent permeability against the inverse mean effective flow pressure were discarded.

A graphical summary of the dataset is shown in Figure 1. A portion (100) of the 130 samples were used as a training data set for both of the machine learning applications, and in those 5 conventional models which required calibration of one or more constant values in their formulae.

Conventional Permeability Models

A total of seven conventional permeability equations were implemented on the dataset to compare with the results of the machine learning methods. The first is based on one of the earliest permeability models proposed by Kozeny (1927), and modified later by Carman (1937). The modified equation is commonly written (e.g., Glover et al., 2006) as

$$k_{Kozeny-Carman} = \frac{cd_g^2\phi^3}{(1-\phi)^2} \quad , \tag{1}$$

where ϕ is porosity, d_g is the mean grain size in μm, and c is a constant. Though commonly used, the Kozeny-Carman relationship has been superseded by other models due to its inability to take account of dead-end pores (Walker and Glover, 2010). The constant is usually found empirically, though some 'standard' but often erroneous values have been published.

Table 1. Statistical summary of the limestone dataset used in this work.

	Porosity (-)	Formation resistivity factor (-)	Characteristic pore throat diameter (m)	Permeability (mD)
Maximum	0.265	200	2.27×10^{-7}	0.185
Minimum	0.107	17	3.92×10^{-10}	1.917×10^{-6}
Arithmetic mean	0.179	62.3	2.88×10^{-8}	0.00525
Standard deviation	0.0371	29.6	4.06×10^{-8}	0.0202
Skewness	0.264	1.56	2.85	6.73

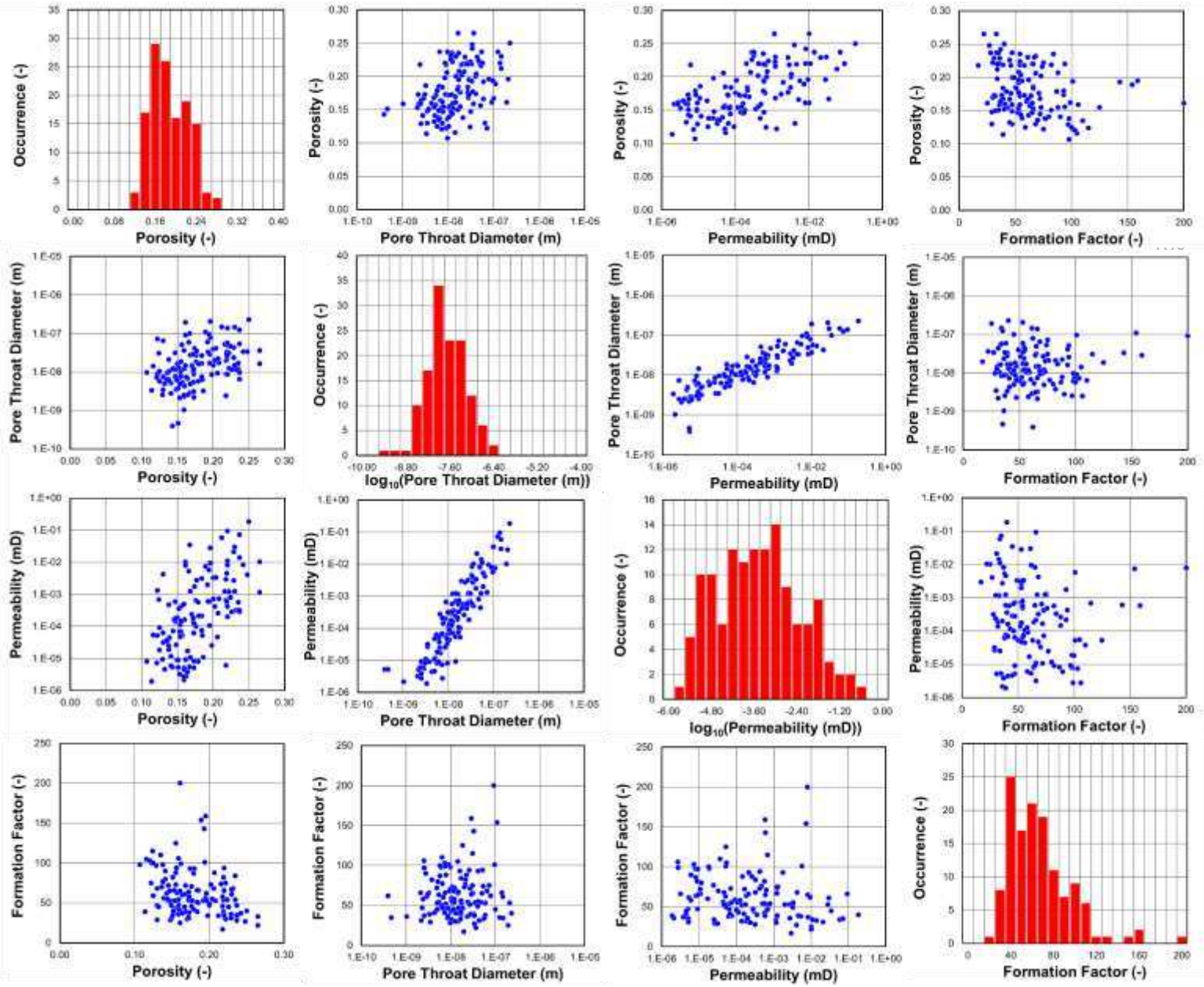

Figure 1. Graphical view of the Portland dataset. Histograms of parameters are shown on the diagonal, while the cross-plots describe the strength of correlation between parameters. Note the logarithmic transformation applied on some parameters in this figure. ***Phi*** = total (He) porosity, ***dPT*** = pore throat diameter (m), ***F*** = Formation Factor, ***K*** = Klinkenberg-corrected pulse-decay permeability (mD).

The second equation is that of Berg (1975), which is

$$k_B = 8.4 \times 10^{-2} d_g^2 \phi^{5.1} , \quad \textbf{(2)}$$

where the permeability is in m^2, while the porosity ϕ is fractional, and d_g is the mean grain diameter in meters. This model was derived empirically from a mixed dataset including carbonates, but not containing tight carbonates. Consequently, this model was not expected to perform well in tight carbonates (Rashid et al., 2015b), an expectation that was borne out in the results.

A similar equation was derived empirically by Van Baaren (Van Baaren, 1979)

$$k_{VB} = 10 d_d^2 \phi^{(3.64+m)} B^{-3.64} , \quad \textbf{(3)}$$

where d_d is the dominant modal grain size in metres, m is the cementation exponent, and B is a sorting index, which is equal to 0.7 for extremely well sorted grains, and unity for extremely poorly sorted grains (Glover et al., 2006). Since the sorting index is unknown here, it was treated as an empirical parameter to be found from fitting the training data.

Unlike the previous three empirical models, the RGPZ equation is an analytically-derived permeability model based on electro-kinetic theory (Glover et al., 2006). This model has both an approximate and an exact form (Glover et al., 2006; Rashid et al., 2015a; 2015b)

$$k_{RGPZ-approximate} = \frac{d_g^2 \phi^{3m}}{4am^2} , \quad \text{and} \quad \textbf{(4)}$$

$$k_{RGPZ\_exact} = \frac{d_g^2}{4am^2 F(F-1)^2} , \quad \textbf{(5)}$$

where k is in m^2, ϕ is porosity, d_g is the grain size in meters, m is the cementation exponent, a is a constant equal to 8/3 for spherical grains, and F is the formation resistivity factor. The approximate form can be used only if F>>1, which for the purposes of the model practically means F>20. Since all tight rocks will conform to this limitation, the approximate form of the RGPZ equation should perform as well as the exact form.

Rashid et al. (2015b) proposed a modified form of the original RGPZ equation to account for the fact that carbonate pores are less connected than pores in sandstones. The resulting modified RGPZ equation for carbonates includes a multiplier η which is carbonate microstructure-dependent. The addition of this multiplier essentially converts Eqs. (4) and (5) into empirical relationships with η as a fitting parameter (Rashid et al., 2015a; 2015b)

$$k_{RGPZ-carbonate} = \frac{d_g^2}{4am^2 \eta F(\eta F-1)^2} . \quad \textbf{(6)}$$

The multiplier η is expected to depend upon the extent and timing of different diagenetic processes as each seeks to modify the pore network architecture in its own way. Consequently, the value of the multiplier η is expected to be useful in trying to quantify the effects of competing diagenetic processes in the control of reservoir quality.

Rashid et al. (2015b) also proposed a new equation which relates permeability to the grain size d_g, and the formation resistivity factor F

$$K_{Generic} = \frac{d_g^2}{bF^3} \ , \tag{7}$$

where b is an empirically-derived fitting parameter. This permeability equation conforms to the general form of permeability equations which is discussed in Walker and Glover (2010).

Permeability Prediction & Machine Learning

The prediction of permeability is a relatively simple case of what is known in machine learning and statistics as regression (Vapnik, 1999; Cuddy and Glover, 2002). Difficulties only arise because (i) the predicted permeabilities are very small (Nazari et al., 2019), (ii) the accuracy of input parameters, whether it be training or test parameters can be low (Rashid et al., 2015b), and (iii) the input parameters are not independent in a complex and often unknown way. Regression is a supervised learning approach where the computer program learns from a set of training input data to estimate or predict the value of a new observation of continuous variable type. The machine learning software allows the computer to reach some learned state on the basis of training data which contains both measurable parameters that may or may not be directly related to permeability, and measurement of the permeability itself (Cuddy and Glover, 2002). The application of that learned state to new data results in a predicted permeability, which should be compared against independent measurements of permeability for the purposes of validation, as in this paper. However, in general use the predicted results would not be checked in such a way, or may perhaps be checked occasionally.

There are many types of machine learning algorithms. A non-exhaustive list of the main types would include (i) naive Bayes classifiers, (ii) nearest neighbour classifiers, (iii) support vector machines (Cortes and Vapnik, 1995) (iv) decision trees, (v) boosted trees, (vi) random forests, (vii) artificial neural networks (ANNs) (Cuddy and Glover, 2002; Yarveicy et al. (2018), and (viii) genetic algorithms (GAs) (Cuddy and Glover, 2002). Most of these, and other machine learning algorithms come in various different types. For example, a type of support vector machine allowing robust least-squares fitting, called the least-squares support vector

machine (LSSVM) is described and used by Yarveicy et al. (2014), and has been applied in the field of petroleum and natural gas engineering successfully by number of authors (Eslamimanesh et al., 2012; Farasat et al., 2013; Rafiee-Taghanaki et al., 2013; Shokrollahi et al., 2013; Ghiasi et al., 2014).

This paper compares the efficacy of using ANNs and GAs to predict the permeability of tight carbonate rocks, in a similar way that Yarveicy and Ghiarsi (2017) compared the efficacy of the extremely randomised trees approach and the LSSVM approach to modelling gas hydrate phase equilibria. Yarveicy et al. (2018) have also carried out comparative studies using ANNs, LSSVMs, adaptive neuro-fuzzy inference systems (ANFIS) and adaptive boosting classification and regression trees (AdaBoost-CART) to predict equilibrium in carbon dioxide/water/Piperazine system, finding that the latter was by far the better approach in this particular system.

In addition, this paper also compares machine learning approaches with seven conventional permeability prediction equations.

Artificial Neural Networks

Artificial neural networks are models which mimic the ability of the brain to learn and solve extremely diverse problems. There are many types of such a model, and the one used here is the Feed Forward Multilayer Perceptron Network (MLPN), which is commonly used for nonlinear regression (Hagan et al., 2014). This type of network consists of an input layer which includes the input parameters. In this work three input parameters were used; the porosity ϕ, the pore throat diameter d_{PT} and the formation factor F.

There is also an output layer which provides the output of the network, and which is the logarithmically-transformed predicted permeability. Between the input and output layers there exists at least one hidden layer as shown in Figure 2. The basic unit of a neural network is called the artificial neuron, which completely or partially composes one layer. The function of each neuron is to sum all incoming signals, together with a bias value. After the summation, a transfer/activation function is applied to the sum before the signal is transmitted to other neurons, in a different layer.

Before it can be deployed to predict permeability, a neural network must be trained. During this training process the network's internal model parameters are adjusted to optimize the network's output by reducing the difference (or error) between the output of the neural network and the reference data (the training permeability in our case). These internal model parameters

are the weighting factors connecting the neurons together and the bias values. The overall process of training progressively reduces the error between the network output and the reference (measured) values (Negnevitsky, 2002; Hagan et al., 2014). There are many training methods such as stochastic learning and gradient descent learning (Rajasekaran and Pai, 2003). The algorithm used here is Adam, one of the most efficient general purpose stochastic learning algorithms which has been introduced and described in detail by Kingma and Lei Ba (2015). The complexity of the neural network model is influenced by its size, i.e., the number of neurons and hidden layers. Bearing in mind the principle of Occam's razor, a network needs to have enough complexity to model the patterns inherent in the data, yet not be so complex that it attempts fitting any random noise that will occur to some extent in any dataset (Hagan et al., 2014).

Figure 2 shows the neural network structure adopted in this case study, and was optimised by experimentation with different structures. The adopted structure is simple but also efficient in capturing the inherent patterns in the data. It consists of a single neuron in each of two hidden layers.

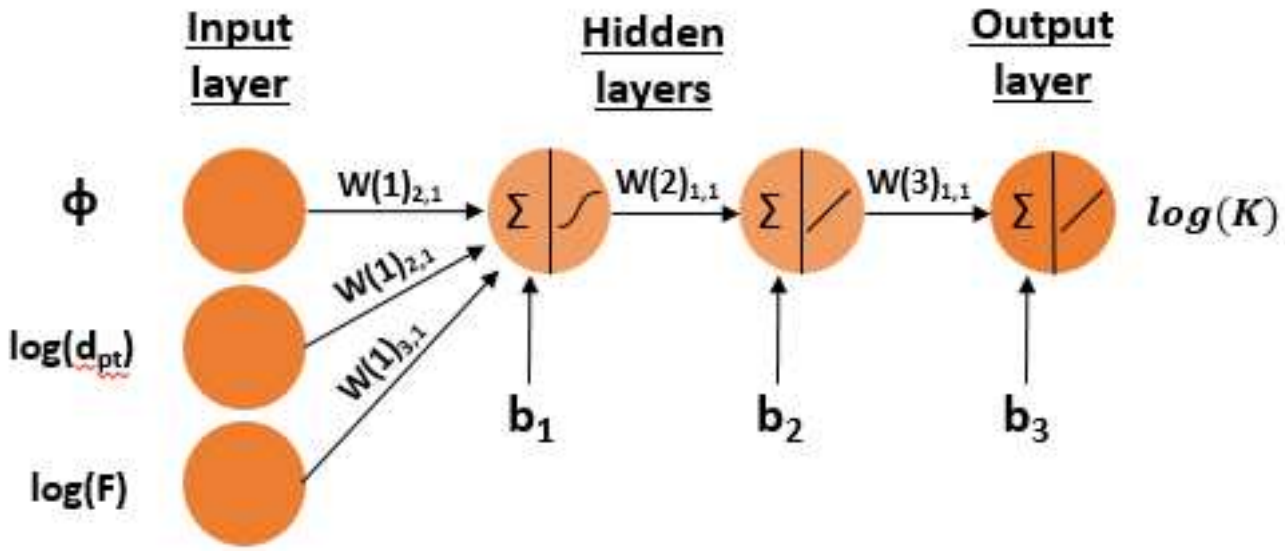

Figure 2. The MLPN structure which has been used in this work. There is one hidden neuron in each of the hidden layers. The transfer function in the first hidden layer is a sigmoidal function while the transfer function in the second hidden layer and the output layer are linear functions.

It is known that artificial neural networks perform better when their parameters are distributed normally or quasi-normally (Hagan et al., 2014). Many of the used parameters are naturally normal or quasi normal. However, some, such as measured permeability follow a log-normal distribution. These parameters were transformed so they resembled a normal distribution more closely so that the modelling could take place. The results of the neural network modelling can be transformed back to a lognormal distribution.

Genetic Algorithms

Genetic algorithms optimize fit to a pattern by simulating the process of natural selection. In this process the most successful 'organisms' from a population survive to pass their genes on to their progeny (Cuddy and Glover, 2002). The chance of survival is related to certain characteristics of the organism which can be passed on to the next generation and/or mutated. Consequently, some of their progeny inherit those characteristics from their parents which improve their survival.

In the genetic algorithm method, the starting point is a population of 'organisms' which, in this specific case represent prediction equations. These 'organisms' have randomly allocated genes, which contain the information required to reconstruct each permeability prediction equation. The most successful equations, defined as those which are best at predicting the permeability of a training set of data, are allowed to partially swap their genes, in the hope that their 'progeny' become even more successful. Random mutations are also allowed at a probability which serves to enhance the diversity of the genetic information of the population (Aminzadeh and De Groot, 2006).

The genetic algorithm technique has been used successfully in the search for suitable empirical permeability prediction equations (e.g., Cuddy and Glover, 2002, Fang et al., 1992). Its particular strength is that it is able to suggest the form of a prediction equation as well as its various coefficients. In our application, the objective is to predict permeability from porosity, pore throat diameter and formation factor. The general equation for the empirical relationship that would have the ability to predict permeability from these three input parameters can be written as

$$k = f(\phi, d_{PT}, F) = [a\ \phi^{b}]\ \bullet_1\ \left[c\ {d_{PT}}^{d}\right]\ \bullet_2\ [e\ F^{f}]\ \bullet_3\ [g]\ , \qquad \textbf{(8)}$$

where k is permeability. The coefficients and exponents are denoted as letters a, b, c, d, e, f and g, all of which have continuous values, and the entities represented by $\bullet_1$, $\bullet_2$ and $\bullet_3$, which are

operators that can be either multiplication or addition. It should be noted that subtraction and division are not required as these operations are taken account of by negative values of the coefficients and exponents. These 10 parameters can be written in the form shown in Figure 3, which is called a 'chromosome', and can be manipulated in the same way as a biological chromosome.

Figure 3. Representation of the permeability equation using a 'chromosome'.

Different types of encoding can be used in genetic algorithms (Rajasekaran and Pai, 2003). The type used in this work is 'value encoding', which implies the use of actual values for the numerical parameters, while binary encoding is used for the two types of operators; multiplication and addition.

In this implementation, a genetic algorithm starts with a randomly generated population of permeability prediction equations, encoded by their chromosomes. All the permeability prediction equations are tested for their goodness of fit to the real data represented by the training dataset. Those that perform well are allowed to survive in a mutated form, and retested against the training dataset. A large number of iterations can be carried out, with the prediction equations becoming more and more precise in their permeability predictions. The processes stopped when a given prediction accuracy is reached.

The survival of permeability prediction equations is judged on the calculation of a 'fitness to survive' parameter, which is higher for equations that provide a smaller prediction error. Two successful permeability prediction equations are then chosen at random to reproduce using their successful genetic information. The genetic information of all new progeny is also subjected to random mutation at a certain probability (Rajasekaran and Pai, 2003). In this type of genetic algorithm, the random mutation was achieved by multiplying the chromosomal numerical values by a random number between 0.8 and 1.2 and flipping the binary code for the operators (Cuddy and Glover, 2002). When run reiteratively, the solution improves over generations until no major improvement can be achieved, and by then the solution can be considered to be converged (Negnevitsky, 2002). The equation corresponding to the

chromosome having the highest fitness among the last generation is selected for being the solution model because it has the highest predictive power.

Results and Discussion

The full dataset of 130 samples was divided at random into two subsets. The first subset, comprising 100 samples, was called the training data subset. This was used to train machine learning techniques and to calibrate those conventional models which required tuned empirical parameters. The second subset comprised 30 samples, and was called the test data subset. This was used to test the efficacy of both the machine learning techniques and the conventional prediction equations.

Conventional models

Figure 4 shows the permeability predicted using each of the benchmark conventional models as a function of the measured permeability. Of the conventional models, the Berg model performed the worst because this model has an empirical origin that is not calibrated for tight carbonates but for the clastic dataset for which it was originally developed. Consequently, its empirical coefficient of 8.4×10^{-2} is fixed. If this value were allowed to vary and to be used as a fitting parameter, it would provide an improved solution.

The other models provided very good results over almost 6 orders of magnitude, especially the various forms of the RGPZ model and the Generic models, which are either purely analytical (RGPZ-exact and the RGPZ-approximate models), or empirical (RGPZ-carbonate and Generic models). Table 2 contains the coefficient of determination and RSME values for the training and test datasets associated with each implementation, as well as the final trained equation.

(Overleaf) **Figure 4.** Permeability prediction using the seven conventional permeability prediction equations, each shown as a function of the independently measured permeability. The whole dataset is split into a training subset and a test subset. Only the Berg equation and the two original RGPZ equations do not require the fitting of at least one parameter to data. For these three, there is no distinction between the training and test data. For the others, their empirical parameters will have been fitted using the training dataset, for which the fit should be optimal, and then applied to the test data, for which the fit should be slightly suboptimal. In each case the uncertainties in each value are approximately the same size as that of the symbols.

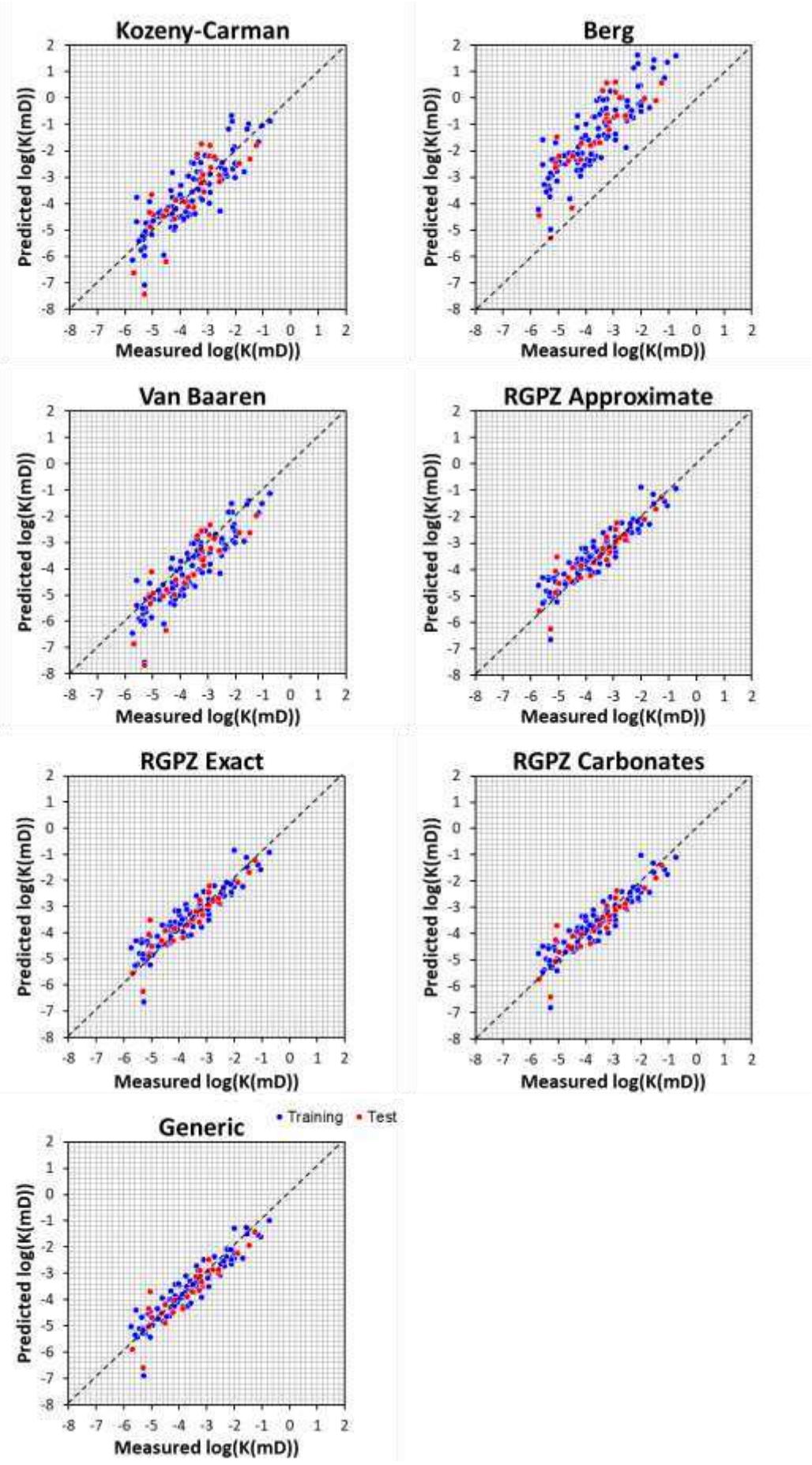
Kozeny-Carman
Berg
Van Baaren
RGPZ Approximate
RGPZ Exact
RGPZ Carbonates
Generic
Training
Test
Predicted log(K(mD))
Measured log(K(mD))
2 1 0 -1 -2 -3 -4 -5 -6 -7 -8
-8 -7 -6 -5 -4 -3 -2 -1 0 1 2

419

Overall the quality of the fits obtained from the conventional models was considered to be very good. This is partly due to the choice of benchmarking conventional models we have used in this paper. There are many other equations, some with a very long pedigree, that would do much worse.

Although this paper concerns itself predominantly with machine learning, it is worthwhile taking away a lesson from the conventional model test that we have done. First, permeability prediction will only be good if it uses input parameters that are of high quality. In this work, we strove to make the highest quality measurements we could. Second, the permeability prediction equation needs to be one which is relevant to the type of rock being predicted. Hence, for tight carbonate rocks, the permeability prediction equation ought to have been developed with tight carbonate rocks in mind. Third, those permeability prediction equations that require fitting to obtain one or more empirical coefficients need to use calibration data sets that contain data for the type of rock being fitted. In our particular case this is tight carbonate rocks, the observation is equally true of other types of rocks.

In all cases, the conventional models which have performed most successfully on tight carbonate rocks are those which have either (i) been specifically designed for tight carbonate rocks, or (ii) have been developed, or had their empirical coefficients determined using datasets containing tight carbonate rocks. In general, good quality prediction can only be expected over a large number of orders of magnitude if the calibration data also extends over a similar range of orders of magnitude. In other words, if the rocks on which one wishes to predict permeability varies from a few μD to hundreds of mD, the calibration of the empirical coefficients needs to be carried out using a dataset which covers the same range.

Neural network models

The optimum network structure for our implementation of the neural network approach was found through experimentation, varying the number of neurons in the hidden layers and observing the response of the objective function. In this work, we found predicting permeability itself does not produce equally good results over the entire range. As some permeabilities are order of magnitude higher than others, the error associated with these far exceeds the error from lower end permeability samples, causing the algorithm to be biased toward predicting the few highest permeabilities as accurately as possible, while disregarding accurate prediction of the lower values. To alleviate this major issue, the root mean squared error (RMSE) of log transformed permeability was implemented as the objective function. This approach has the

advantage of equalizing the contribution of the errors from the entire permeability range. The objective function is given by Eq. (9), where it should be noted that the permeabilities are treated in the logarithmic domain because they are distributed log normally.

$$Objective\ function = \sqrt{\frac{1}{n}\sum_{i=1}^{n}\left(\log\left(K_{predicted}\right) - \log(K_{measured})\right)^2} \quad \textbf{(9)}$$

In our application, it became clear that using larger number of neurons improved the fit of the predicted permeability to the training subset resulting in a lower value of the objective function. However, the accuracy of the subsequent use of the neural network on unseen samples diminished. This is because the neural network was 'over-fitting' the training samples. Overfitting occurs due to the model being too powerful such that it exceeds the requirement of just fitting the patterns in the data, and starts to memorize the training points. This process results in the performance of the model on the training dataset increasing without limit, but such an increase in performance is counter-productive because it occurs at the expense of the model's capability to fit unseen data (Negnevitsky, 2002). Since the training data points are normally noise contaminated, and may not adequately represent the entire population, it is critical to avoid overfitting when deciding on the size of the neural network size to be used. Often simple neural networks perform just as well, and sometimes even better than very complex neural networks.

Figure 5 shows the results of varying the number of neurons for our application with three input parameters: porosity, grain size and formation factor. A network with one neuron in each hidden layer was chosen, giving the smallest value of objective function for the test samples.

The permeability prediction results from the MLPN model are shown in Figure 6, where the predicted permeability is plotted as a function of the measured permeability for both the training and the test data in the dual-logarithmic domain. It is clear from this figure that the neural network provides a very good fit to the measured permeability data over six orders of magnitude.

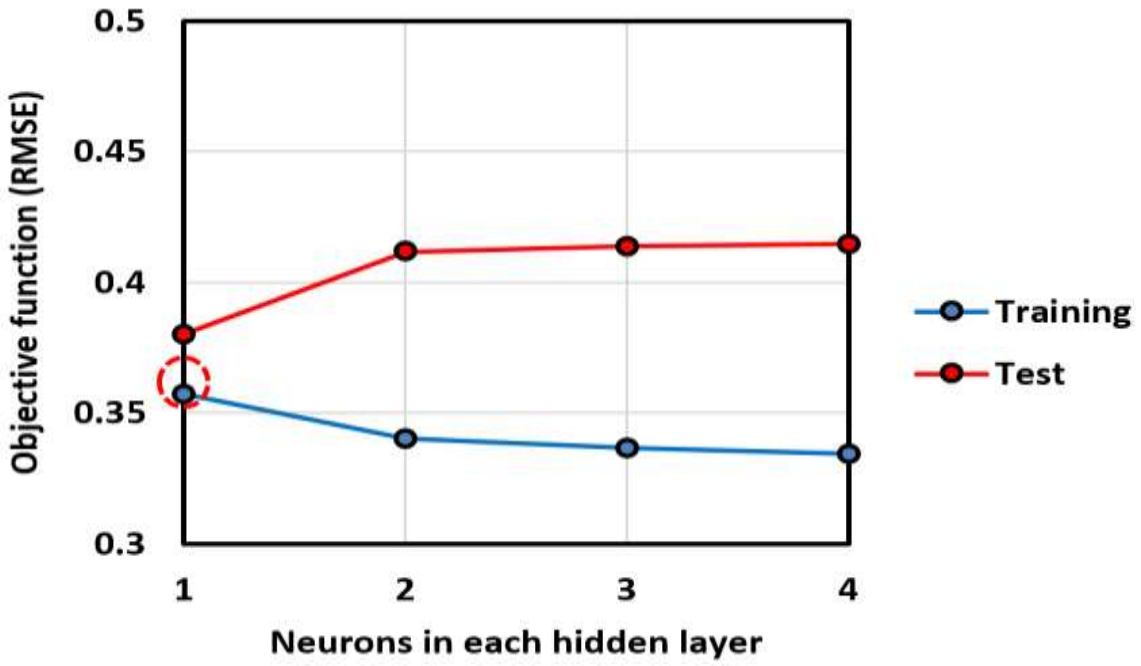

Figure 5. Hyperparameter testing of network size showing that, for this application, a smaller network size is less accurate on the training data but its generalization on unfamiliar samples is more robust.

The permeability prediction results from the MLPN model are shown in Figure 6, where the predicted permeability is plotted as a function of the measured permeability for both the training and the test data in the dual-logarithmic domain. It is clear from this figure that the neural network provides a very good fit to the measured permeability data over six orders of magnitude.

Genetic algorithm models

The permeability prediction results from implementing the genetic algorithm technique are also shown in **Figure 6**, once again with the predicted permeability plotted as a function of the measured permeability for both the training and the test data and in the dual-logarithmic domain. The predicted permeabilities using this technique are also clearly very good compared to most of the conventional models.

The genetic algorithm technique has the advantage of also providing a prediction equation that is tailored to the training dataset. In this case the genetic algorithm technique provides permeability prediction through this equation

$$k = \frac{122365341777308\,\phi^{2.748}\,d_{PT}^{1.864}}{F^{0.6}}, \qquad \textbf{(10)}$$

503 which can be rewritten in a generalized form

504 $$k = \frac{M\phi^a d_{PT}^b}{F^c}, \quad \textbf{(11)}$$

505 which is consistent with Eq. (10), and where M, a, b and c are fitting parameters, whose exact
506 values are sample-dependent and whose mean values are formation-dependent.

507 Equation (11) contains two parameters which are known to be partially correlated. The
508 formation factor F is known to be dependent on both porosity and cementation exponent m
509 through Archie's first law (Archie, 1942), which can be stated as $F = \phi^m$. This equation arises
510 from the fact that electrical flow through a rock with insulating grains occurs only through the
511 conducting fluid occupying the pores. The resistivity of the rock depends on the amount of
512 fluid present, which is given by the porosity and assumes that the pores are completely saturated
513 with the fluid, and also depends on how well that fluid is connected, which is described by the
514 value of the so-called cementation exponent m (Glover, 2015). Consequently, Equation (10)
515 may be rewritten as

516 $$k = 122365341777308\, \phi^{(2.748+0.6m)}\, d_{PT}^{1.864}, \quad \textbf{(12)}$$

517 or generically as

518 $$k = M\phi^{(a+cm)} d_{PT}^b . \quad \textbf{(13)}$$

519 The large value of M in Equation (12) arises solely from the fact that the input parameters
520 for the genetic algorithm model used permeability training data in millidarcies. When
521 converted to m^2, this value becomes 0.0122, which corresponds well to the value for the
522 constant term in the RGPZ equation. This term is $1/4am^2$, and can be calculated for the mean
523 behaviour of the dataset from the data given in Table 1. When the cementation exponent is
524 calculated using Archie's first law from this data, we obtain a mean cementation exponent of
525 m=2.402, which provides a value of 0.0162 for the constant term. Consequently, we conclude
526 that the M term in Equation (12) is consistent with the theoretically-derived RGPZ equation.

527 Considering the other variables in Equation (12), we find that the genetic algorithm method
528 underestimates the porosity exponent compared to the RGPZ equation, providing 2.748+0.6m,
529 which is equal to 4.189 when m=2.402, compared to a value of 3m, which is equal to 7.206 for
530 the RGPZ equation; an overestimation of just over 3. The genetic algorithm method also
531 underestimates the grain size exponent, giving 1.864 compared to the RGPZ equation's value
532 of exactly 2.
533

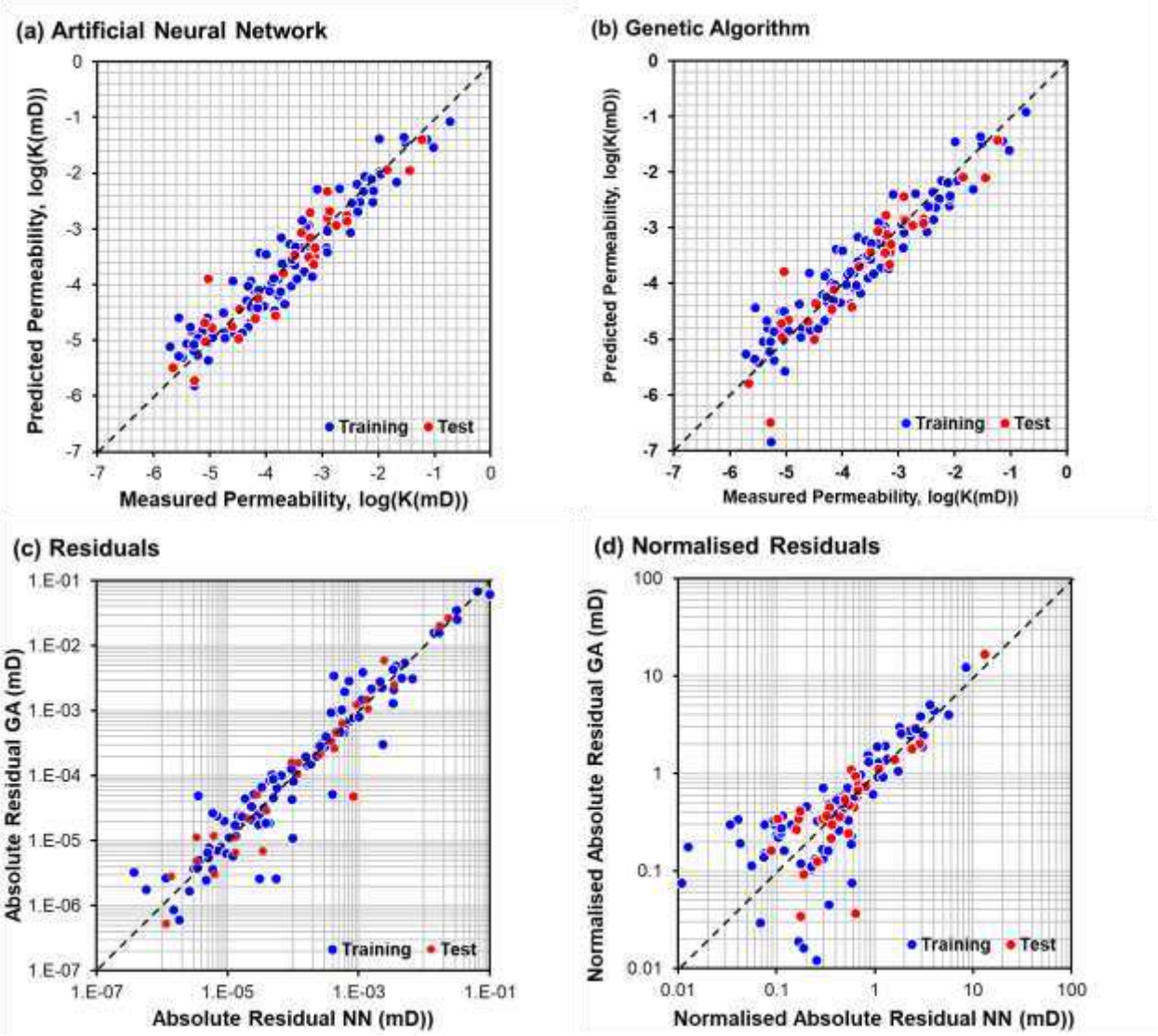

Figure 6. Permeability prediction results for the trained neural network (a) and using the genetic algorithm approach (b), when applied to the training and the test datasets as a function of the laboratory measured permeabilities. (c) Cross-plot of the absolute residuals from the genetic algorithm (GA) method with that from the neural network method. (d) Cross-plot of the normalised absolute residuals from the genetic algorithm (GA) method with that from the neural network method. Almost all the predictions fall within one order of magnitude away from the actual measurements.

Equation (13) gives some insight into the controls on permeability offered by the rock matrix and its microstructure. It implies three main controls on permeability:

1. Porosity. This recognizes that the higher the porosity, the higher the permeability is likely to be. The sensitivity of permeability to changes in porosity is given by what we might now call the sensitivity factor *a* in Equation (13).

2. Connectivity of the pores. This recognizes that high porosities, if unconnected will have zero permeability and for any given porosity permeability will be greater if pore connectivity is higher. The sensitivity of permeability to changes in connectivity is given by what we might now call the sensitivity factor c in Equation (13).
3. The characteristic pore throat diameter. It is an important parameter for permeability since narrower pore throats act like bottlenecks for fluid flow. The sensitivity of permeability to characteristic pore throat diameter is given by what we might now call the sensitivity factor b in Equation (13).

Prediction performance

The error metrics for all predictions are shown in **Table 2** and in Figure 7. Good fits are represented by low values of root mean squared error (RSME) together with high values of coefficient of determination (R^2). The quality of the predictions is far from uniform. Even with their historic success on conventional sandstone reservoirs, the older empirical models were not successful on these tight carbonate rocks. The RGPZ-carbonate equation provided the best fit from the conventional approaches, with the lowest RMSE error of 0.458. The other RGPZ equations performed slightly worse as they do not include the carbonate calibration parameter η, but nevertheless provided acceptable predictions. The genetic algorithm solution performed marginally better than the rest of the conventional equations, with an RMSE of 0.433. On the other hand, the artificial neural network technique provided the most accurate predictions with an RMSE of only 0.380.

The marginal difference between the two machine learning approaches arises from only a few data points. Reference to Figure 6 shows that there are two data points, one in the training dataset and another in the test dataset whose permeabilities are underestimated by one order of magnitude. The reason why these particular points are not predicted well is not currently known. However, we carried out a sample by sample comparison of both machine learning approaches, and find that the prediction error for the genetic algorithms correlates with the prediction error. Figure 6c shows a cross-plot of the absolute residuals from the genetic algorithm method (GA) against that from the neural network (NN) method. It is clear that samples whose permeability is badly predicted by one method is also badly predicted by the other, with correlation coefficients of 0.963, 0.994 and 0.962, for the training dataset, test dataset, and combined datasets, respectively. We recognise that this comparison might be biased towards large permeability measurements due to the large range of permeabilities used

581 in the study. The large range of permeabilities covered in the prediction might lead to small
582 percentage errors in large permeabilities being given more weight than large percentage errors
583 in small permeabilities. Hence, we also show the cross-plot of the absolute residuals normalised
584 by the measured permeability, which is shown in Figure 6d. Once again, the normalised
585 absolute residuals correlate well, with coefficients of correlation of 0.945, 0.991 and 0.969, for
586 the training dataset, test dataset, and combined datasets, respectively. In Figure 6d, the abscissa
587 x=1 and ordinate y=1 represent an error in prediction of the same magnitude as the measured
588 permeability (i.e., a ±100% error) for the neural network and genetic algorithm methods,
589 respectively. Those points with coordinates (x,y) > (1,1) represent predictions by both
590 techniques that are very much in error, and for these the degree of bad prediction in one
591 machine learning method is similar to that in the other. For those points where the prediction
592 is better, i.e., (x,y) < (1,1), there is more scatter indicating that one method produces a better
593 prediction than the other.
594 From the analysis above we infer that the lack of prediction accuracy is not predominantly
595 a function of the technique being used, but due to a problem with the input parameters. There
596 are two possibilities here: (i) that non-systematic errors in one or more of the input parameters
597 leads to both machine learning techniques badly predicting some of the samples, and (ii) the
598 permeability of the tight carbonate rocks depending upon some petrophysical characteristic
599 that is not characterised sufficiently by any of the input parameters used in this study. An
600 example of the latter might be that the permeability is dependent upon the rock wettability, but
601 none of the input parameters include information about rock wettability. Further work would
602 need to be carried out in order to ascertain whether this was the case.
603 We note, however, that the few samples for which the predictions were worst have a
604 different structure from the rest of the dataset in that they have a high permeability but a low
605 porosity and a small pore throat size. From such parameters, we infer that the pore space that
606 is present must be highly connected. Samples with this type of microstructure occur when the
607 diagenetic process of cementation has occluded original pore volume, reducing the size of the
608 throats connecting the pores as well as the pores themselves, but leaving the remaining flow
609 paths highly connected. Examples of such behaviour can be found in Fontainebleau and
610 Lochaline sandstones (Walker and Glover, 2018) and in carbonates (Rashid et al., 2015a;
611 2015b, 2017). The inefficiency of the machine learning techniques stems from the relative lack
612 of samples with this type of structure in the training dataset. The permeability is predicted badly
613 precisely because the machine learning techniques have not been prepared to recognise samples
614 with this type of pore microstructure. It is a sobering thought that any machine learning

algorithm is only as good as the quality of the data with which it is trained and upon which it is applied.

It is worth noting that the fits by empirical equations and machine learning implementations are slightly better for the training dataset than the test dataset. This is due to the chance that the models are calibrated on a sample that is not quite representative enough of the characteristics of the formation. Besides this, there is also a chance of inclusion of two outliers in the test dataset that reduces the efficacy of all the models in the test dataset.

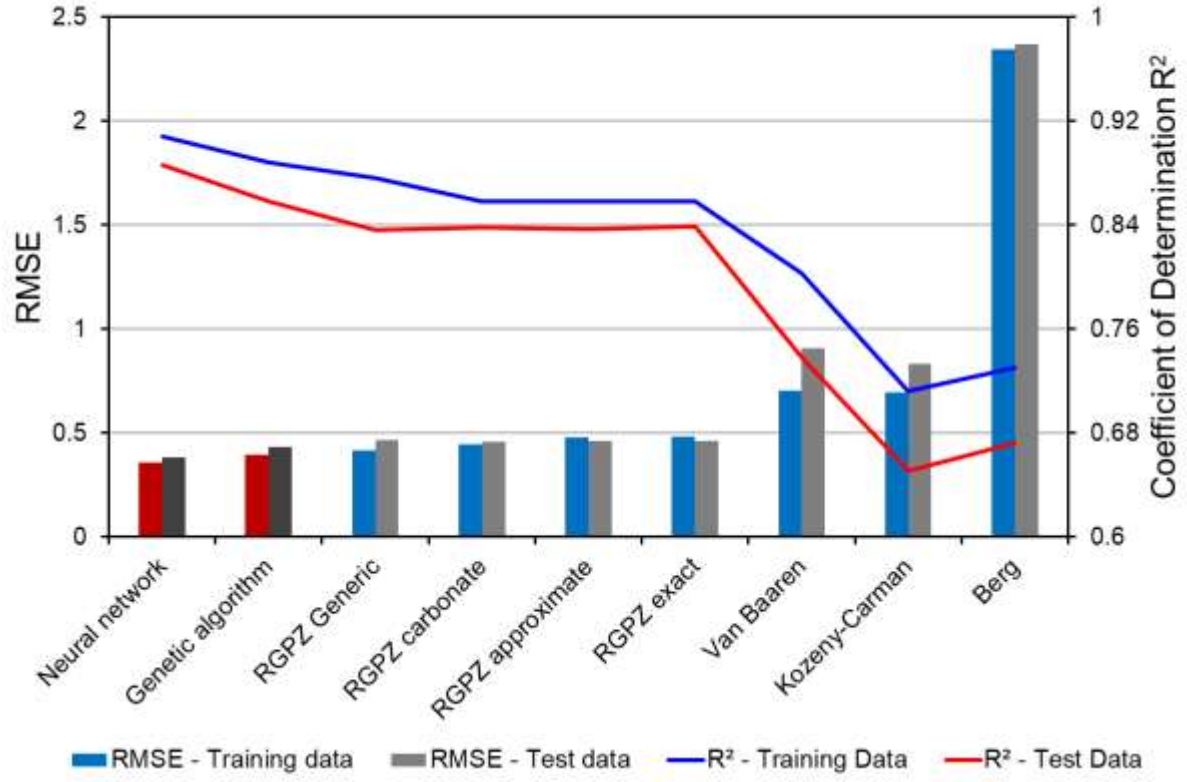

Figure 7. Permeability prediction metrics for all conventional and machine learning techniques for the training and test datasets.

Table 2. A summary of accuracy measures for the permeability prediction solutions for the Portland limestone, arranged in order of performance, best first.

Permeability Model	Trained equation/model	Training subset		Test subset	
		RMSE	R^2	RMSE	R^2
Feed forward multilayer perceptron network	A fitted model as following: $N1=[-0.37531\times\phi-2.19641\times\log(d_{PT})+0.30725\times\log(F)]+0.61237$ 1st neuron output$=1/(1+e^{-N1})$ 2nd neuron output$=-0.8194\times A1+0.33022$ $\text{Log}(k)=2.7881\times$2nd neuron output$+0.22452$ Input and output parameters are normalized to a range of -1 to 1	0.357	0.908	0.380	0.886
Genetic algorithm	$122365341777308\ \phi^{(2.748+0.6m)}\ d_{PT}^{1.864}$	0.394	0.888	0.433	0.858
RGPZ carbonate	$\frac{d_g^2}{4am^2\eta F(\eta F-1)^2}$ where $\eta = 1.15$	0.445	0.858	0.458	0.838
RGPZ approximate	$\frac{d_g^2\phi^{3m}}{4am^2}$ *	0.476	0.858	0.461	0.837
RGPZ exact	$\frac{d_g^2}{4am^2F(F-1)^2}$ *	0.482	0.858	0.462	0.839
RGPZ Generic	$\frac{d_g^2}{83.72F^3}$	0.415	0.876	0.467	0.836
Kozeny-Carman	$\frac{8615961931d_g^2\phi^3}{(1-\phi)^2}$	0.696	0.712	0.833	0.651
Van Baaren	$10d_d^2\phi^{(3.64+m)}0.001^{-3.64}$	0.704	0.803	0.907	0.738
Berg	$8.4*10^{-2}d_g^2\phi^{5.1}$ *	2.344	0.73	2.368	0.672

* These equations are not calibrated but are fixed empirical (Berg) or theoretically derived equations (RGPZ approximate and RGPZ exact).

The results presented in this paper show that the implementation of genetic algorithms and artificial neural networks results in more accurate predictions in comparison to predictions made by all the benchmark permeability models including the most recent ones. The genetic algorithm technique helped reduce the error of the best performing conventional permeability model by 5%. On the other hand, the artificial neural networks technique reduced the error by 17%, which is a significant improvement. On the other hand, the solution of the neural network approach, which is something of a 'black box', is not as transparent as the trained equation provided by the genetic algorithm method. The representation of the solution in a concise mathematical equation provides a much clearer insight into the significance and role of each input parameter into the permeability prediction. Also, the resulting equation can be applied more easily to similar facies without the need for special software and/or technical skills. The solution equation can also be recalibrated with a small number of samples because of the smaller number of model parameters.

By contrast, the permeability prediction using artificial neural networks is mathematically more complex. While it is simple to visualize the solution of a neural network that has a single input feature on a *xy* graph, to visualize it when two input parameters are used requires a three-dimensional plot. Nonetheless, visualizing the response of networks that use multi-dimensional input features is indeed challenging.

Limitations of machine learning

The main result of this study is that both the machine learning techniques tested performed better than all of the conventional permeability equations over a range of 6 orders of magnitude. There are, however, some important limitations of machine learning which need to be considered before blindly applying them.

The first is that it can be simple to fall into the trap of creating neural networks which are too complex, and which will seem to be doing a good job of permeability prediction on the training data, but which lead to over-training. Such models will not perform as well on the target dataset, and that partial failure will not be clear because independent permeability measurements will not be available. Why, after all, predict permeability if one already knows it.

The second is that both techniques are to some extent a black box, although that is less true of genetic algorithms. Consequently, if there is a failure in the techniques, it is not always clear to the operator.

663 Third, both techniques need training. The training dataset must be a random sample of the
664 whole population on which the technique is to be used. This is not just the trivial constraints
665 that the sampling should be truly random, of sufficient number to capture all of the complexities
666 in the target data, and covering the same range of measurements in the same proportion. By
667 definition, rare events, conditions and outliers in general will be lost from the analysis. Machine
668 learning is in a certain light, a form of conservative filtering that keeps the common and rejects
669 the rare. Consequently, machine learning will fail to predict rare but important values.
670 The fourth limitation concerns the interpretation of what is a good genetic algorithm result.
671 If there are sufficient organisms evolving, it is reasonable that one of the most successful will
672 provide the permeability prediction equation that is the most appropriate. We use the words
673 'most appropriate' deliberately, because it will not necessarily be the best. The set of successful
674 chromosomes, however numerous and however statistically defined are non-unique. In other
675 words, two chromosomes which are very different could provide equally good results. How is
676 one then to choose which to use on a set of target data, where the accuracy of the result cannot
677 be tested.
678 In summary, no matter how well-implemented, the use of machine learning will always be
679 associated with some anxiety that the predictions are as good as we have found. If that anxiety
680 is such that the final results always need to be validated by some independent measure of
681 permeability, the utility of the approach is weakened.
682
683 **Diagenesis and machine learning**
684 As we have seen, both the genetic algorithm and neural network models perform better than
685 the best of the theoretical and empirical models. It is instructive to examine the reasons for this
686 in tight, often diagenetic altered, carbonate rocks. Conventionally, the spread in a poroperm
687 diagram is attributed to the permeability depending upon factors other than porosity. However,
688 many of the theoretical and empirical models presented in this paper include a range of other
689 parameters, including, for example, grain size, formation factor and cementation exponent but
690 still result in a suboptimal prediction of permeability. This is because the permeability is some
691 additional function of a parameter that is not included in the structure of the prediction equation,
692 or that there is a lack of orthogonality between the input parameters. The defined structure of
693 the prediction equation limits the efficacy of the model to predict permeability in only those
694 rocks where the imposed structure is valid, i.e., simple functional dependencies of a limited
695 number of known input parameters.

Here, both machine learning techniques perform better than all the conventional approaches, so we can infer that they have a common ability to make better use of the available data than conventional predictive equations. The common characteristic of the two machine learning methodologies used in this work, as well as all machine learning approaches, is that they start with either no structure or relatively little structure. The neural networks have only defined input and output values, while the genetic algorithm has input and output values as well as a very generalised equation. In machine learning, structural complexity arises from training and is theoretically only limited by the availability of a representative training dataset. Consequently the result of complex interacting processes should be modellable with accuracy.

The permeability of tight carbonate rocks is the result of the complex, interacting process of diagenesis. Hence, we hypothesize that the permeability of rocks which have undergone diagenesis would be ideally suited to machine learning methods, whose greater sensitivity to subtle and complex changes in the input parameters can be taken into account.

Of all of the conventional models, it was the carbonate version of the RGPZ model that came closest to the machine learning models. This model includes the η parameter, which is supposed to take account of the fact that the pore network architecture in carbonate rocks is more complex than that in clastic rocks (Rashid et al., 2015b). However, a single value, set to η=1.15 in this work, is a very crude method for taking account of the pore network which will have a connectedness that may depend upon codependent and competing processes of compaction, cementation, vug formation, dissolution, dolomitisation and fracturing.

Figure 8 shows a generic poroperm cross plot implemented for the modified carbonate RGPZ model for four different grain sizes. The superimposed arrows (which are imposed at an arbitrary point on an arbitrary curve, but are equally relevant to any point on any of the curves) show the approximate directions each diagenetic process will produce when acting upon the pore network architecture of a carbonate rock. None of the arrows follow the curves, because that would indicate that the process was not altering either the rock matrix or the pore network architecture. The transparent grey areas in the figure are an indication of those where gain or loss in porosity leads to a loss or gain in permeability. There are however no diagenetic processes which cause such tendencies.

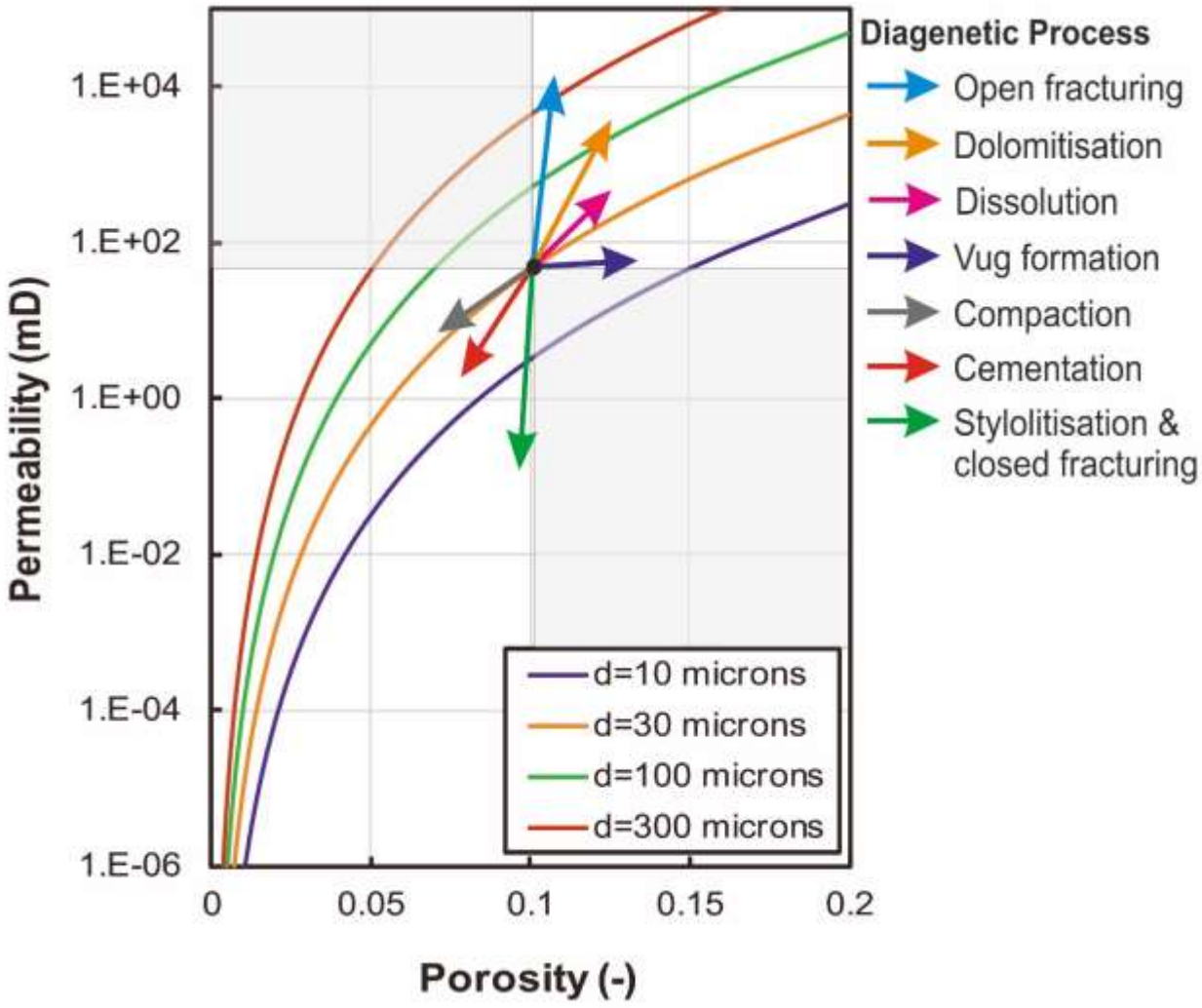

Figure 8. Diagrammatic poroperm cross-plot based on the modified carbonate RGPZ model for grain sizes. The arrows, which all originate at an arbitrary point on one of the curves, but equally well apply to any point on any of the curves, represents the results of different diagenetic processes altering the pore network architecture of the rock and hence its porosity and permeability characteristics. High reservoir quality occurs towards the top right of the figure.

Compaction (grey arrow) reduces porosity, but can result in less permeability loss than expected depending on the sorting, shape and strength of the grains. Cementation (red arrow) results in loss of porosity as cement fills the pore spaces, and significant loss of permeability because the cement will either partially or totally occlude pore throats, hence blocking fluid flow pathways. By comparison, dissolution (magenta arrow) tends to dissolve rock matrix indiscriminately, increasing porosity but not preferentially in the pore throats. Consequently, though mobility does increase, it does not do so significantly. Dolomitisation (orange arrow) has a much greater effect because the recrystallisation concomitant upon dolomitisation provides larger porosity within pores that are well connected, and hence support much greater

743 permeability. Vug formation (dark blue arrow), for example by preferential dissolution,
744 introduces significant porosity. However, this porosity is often distributed in an unconnected
745 manner in a background matrix of low permeability, and hence results in very little increase in
746 permeability. Stylolitisation (green arrow) has negligible impact upon the porosity of a rock,
747 but by concentrating clay minerals along the stylolite surface, the macroscopic permeability of
748 the rock perpendicular to the stylolites is greatly reduced. Since stylolite form perpendicular to
749 the direction of greatest principal stress, this direction is usually vertical. Fracturing (light blue
750 arrow), of course, introduces very little extra porosity to a rock, but that porosity is arranged
751 for the efficient transport of fluid in the direction of the fractures. Consequently, porosity
752 increases slightly upon fracturing, but permeability in the direction of the fractures can increase
753 by two or more orders of magnitude if the fractures are open. If the fractures are closed, the
754 trend would be very similar to that for the stylolites, with the closed fractures providing a
755 similar compartmentalised single role.

756 Taking all of these diagenetic factors in consideration, it is unlikely that the η parameter
757 would be able to take account of all of the diagenetic controls on permeability provided by
758 these codependent and competing diagenetic processes. However, the training of either a new
759 network or genetic algorithm on a reasonable size training dataset would be likely to result in
760 a model that takes account of the main controls of diagenesis on permeability.

761 Finally, we recognize that the true novelty of this paper is not that it tests two machine
762 learning methodologies for the first time on a high-quality, well-characterised tight carbonate
763 system, but the recognition that the quasi-quantitative parameters obtained from these
764 techniques may contain information which will help us improve the quantitative analysis of the
765 type and extent of diagenesis with regards to its control on rock permeability.

766

767 ## Conclusions

768 In this work, both artificial neural network and genetic algorithm techniques have been
769 demonstrated to show potential for the prediction of technically challenging tight carbonate
770 reservoirs. The genetic algorithm technique is more useful if one wishes to gain more insight
771 into which parameters are controlling the predicted permeability, and has the benefit of
772 providing an equation that can be subsequently applied easily to other datasets or used as the
773 starting point of training with another dataset. However, when accuracy is the top priority, the
774 neural network technique was found to be more accurate.

We have considered the reasons for the machine learning techniques providing a better predicted permeability compared to the conventional models, considering that some of the conventional models are very high quality and contain the same parameters used in machine learning approaches. We have concluded that the better performance of machine learning techniques over conventional approaches can be attributed to their enhanced capability to model the connectivity of pore microstructures using a significant training dataset. This allows machine learning methods to take account of small changes in pore microstructure caused by the complex, codependent and competing diagenetic processes that have conspired to create the pore microstructure of any given carbonate rock. In doing so, we have created a qualitative model which describes how the poroperm characteristics of tight carbonate rocks are modified by each of eight diagenetic processes.

We conclude that, for tight carbonate reservoirs, both machine learning techniques predict permeability more reliably and more accurately than conventional models and may be capable of distinguishing quantitatively between pore microstructures caused by different diagenetic processes.

Acknowledgements

The authors would like to thank two anonymous reviewers, whose incisive and constructive comments have improved this paper greatly.

References

AKAI, T., TAKAKUWA, Y., SATO, K. & WOOD, J. M. 2016. Pressure Dependent Permeability of Tight Rocks, 180262-MS SPE Conference Paper – 2016.

AL-ZAINALDIN, S., GLOVER, P.W.J. and LORINCZI, P., 2017. Synthetic Fractal Modelling of Heterogeneous and Anisotropic Reservoirs for Use in Simulation Studies: Implications on Their Hydrocarbon Recovery Prediction. Transport in Porous Media, 116(1), pp. 181-212.

AMINZADEH, F. & DE GROOT, P. 2006. *Neural networks and other soft computing techniques with applications in the oil industry*, EAGE Publications.

ARCHIE, G. E., 1942, The electrical resistivity log as an aid in determining some reservoir characteristics: Transactions of the American Institute of Mechanical Engineers, 146, 54–67.

BARTON, C.M.; WOODS, M.A.; BRISTOW, C.R.; NEWELL, A.J.; WESTHEAD, R.K.; EVANS, D.J.; KIRBY, G.A.; WARRINGTON, G. 2011. Geology of south Dorset and south-east Devon and its World Heritage Coast : Special Memoir, British Geological Survey, 161 pp.

BERG, R. R. 1975. Capillary pressures in stratigraphic traps. *AAPG bulletin,* 59**,** 939-956.

CARMAN, P. C. 1937. Fluid flow through granular beds. *Transactions-Institution of Chemical Engineers,* 15**,** 150-166.

CORTES, C. & VAPNIK, 1995. Support-vector networks, Mach. Learn., 20, 273. doi.org/10.1007/BF00994018

CUDDY, S. & GLOVER, P.W.J. 2002. The application of fuzzy logic and genetic algorithms to reservoir characterization and modeling. *Soft Computing for Reservoir Characterization and Modeling*. Springer.

KINGMA, D.P. and BA, J.L., 2015. Adam: A method for stochastic optimization, 3rd International Conference on Learning Representations, ICLR 2015 - Conference Track Proceedings 2015.

FANG, J., KARR, C. L. & STANLEY, D. A. 1992. Genetic algorithm and its application to petrophysics.

GHIASI, M.M., SHAHDI, A., BARATI, P., ARABLOO, M., 2014. Robust modeling for efficient estimation of compressibility factor in retrograde gas condensate systems. Ind. Eng. Chem. Res. http://dx.doi.org/10.1021/ie404269b.

GLOVER, P.W.J., LORINCZI, P., AL-ZAINALDIN, S., AL-RAMADAN, H., DANIEL, G. and SINAN, S., 2018. Advanced fractal modelling of heterogeneous and anisotropic reservoirs, SPWLA 59th Annual Logging Symposium 2018 2018.

GLOVER, P.W.J., 2015, Geophysical Properties of the Near Surface Earth: Electrical Properties , 11.03, pp. 89-137, in Treatise on Geophysics (2nd Ed.), Ed. G. Schubert

GLOVER, P.W.J., ZADJALI, I. & FREW, K. 2006. Permeability prediction from MICP and NMR data using an electrokinetic approach. *Geophysics,* 71**,** F49-F60.

ESLAMIMANESH, A., GHARAGHEIZI, F., ILLBEIGI, M., MOHAMMADI, A.H., FAZLALI, A., RICHON, D, 2012. Phase equilibrium modeling of clathrate hydrates of methane, carbon dioxide, nitrogen, and hydrogen + water soluble organic promoters using Support Vector Machine algorithm. Fluid Phase Equilibr. 316, 34-45.

FARASAT, A., SHOKROLLAHI, A., ARABLOO, M., GHARAGHEIZI, F., MOHAMMADI, A.H., 2013. Toward an intelligent approach for determination of saturation pressure of crude oil. Fuel Process. Technol. 115, 201-214.

HAGAN, M. T., DEMUTH, H. B., BEALE, M. H. & DE JESÚS, O. 2014. *Neural Network Design (2nd Edition)*.

HUSSEIN, D., COLLIER, R., LAWRENCE, J.A., RASHID, F., GLOVER, P.W.J., LORINCZI, P. and BABAN, D.H., 2017. Stratigraphic correlation and paleoenvironmental analysis of the hydrocarbon-bearing Early Miocene Euphrates and Jeribe formations in the Zagros folded-thrust belt. Arabian Journal of Geosciences, 10(24).

KOZENY, J. 1927. *Über kapillare leitung des wassers im boden:(aufstieg, versickerung und anwendung auf die bewässerung)*, Hölder-Pichler-Tempsky.

LIM, J.-S. & KIM, J., 2004. Reservoir porosity and permeability estimation from well logs using fuzzy logic and neural networks. SPE 88476.

MA, Y.Z., HOLDITCH, S., and ROYER, J.-J., 2016, Unconventional Oil and Gas Resources Handbook Evaluation and Development, Elsevier, 536 pp., ISBN: 978-0-12-802238-2.

NAZARI, M.H., TAVAKOLI, V., RAHIMPOUR-BONAB, H. and SHARIFI-YAZDI, M., 2019. Investigation of factors influencing geological heterogeneity in tight gas carbonates, Permian reservoir of the Persian Gulf. Journal of Petroleum Science and Engineering, 183.

NEGNEVITSKY, M. 2002. *Artificial Intelligence: A Guide to Intelligent Systems*, Addison-Wesley.

ONALO, D., ADEDIGBA, S., KHAN, F., JAMES, L.A. and BUTT, S., 2018. Data driven model for sonic well log prediction. Journal of Petroleum Science and Engineering, 170, pp. 1022-1037.

ONALO, D., OLORUNTOBI, O., ADEDIGBA, S., KHAN, F., JAMES, L. and BUTT, S., 2019. Dynamic data driven sonic well log model for formation evaluation. Journal of Petroleum Science and Engineering, 175, pp. 1049-1062.

RAFIEE-TAGHANAKI, S., ARABLOO, M., CHAMKALANI, A., AMANI, M., ZARGARI, M.H., ADELZADEH, M.R., 2013. Implementation of SVM framework to estimate PVT properties of reservoir oil, Fluid Phase Equilibria, 346, 25-32, doi.org/10.1016/j.fluid.2013.02.012

RAJASEKARAN, S. & PAI, G. V. 2003. *Neural networks, fuzzy logic and genetic algorithm: synthesis and applications (with cd)*, PHI Learning Pvt. Ltd.

RASHID, F., GLOVER, P.W.J., LORINCZI, P., COLLIER, R., LAWRENCE, J., Porosity and permeability of tight carbonate reservoir rocks in the north of Iraq, *Journal of Petroleum Science and Engineering*, 133, 147-161, 2015a, doi: 10.1016/j.petrol.2015.05.009

RASHID, F., GLOVER, P., LORINCZI, P., HUSSEIN, D., COLLIER, R. & LAWRENCE, J. 2015b. Permeability prediction in tight carbonate rocks using capillary pressure measurements. *Marine and Petroleum Geology,* 68**,** 536-550.

RASHID, F., GLOVER, P.W.J., LORINCZI, P., HUSSEIN, D. and LAWRENCE, J.A., 2017. Microstructural controls on reservoir quality in tight oil carbonate reservoir rocks. Journal of Petroleum Science and Engineering, 156, pp. 814-826.

SEN M.K., MALLICK S. (2018) Genetic Algorithm with Applications in Geophysics. In: Application of Soft Computing and Intelligent Methods in Geophysics. Springer Geophysics. Springer, Cham

SHOKROLLAHI, A., ARABLOO, M., GHARAGHEIZI, F., MOHAMMADI, A.H., 2013. Intelligent model for prediction of CO2 e reservoir oil minimum miscibility pressure. Fuel 112, 375e384.

TANG, H., 2008. Improved carbonate reservoir facies classification using artificial neural network method. Proceedings of the Canadian International Petroleum Conference/SPE Gas Technology Symposium 2008 Joint Conference (the Petroleum Society's 59th Annual Technical Meeting), Calgary, Alberta, Canada, 17-19 June 2008.

TANG, H., TOOMEY,N. and MEDDAUGH, W.S., 2011, Using an artificial – neural – network method to predict carbonate well log facies successfully, SPE Reservoir Evaluation and Engineering, SPE123998, 35-44.

VAN BAAREN, J. Quick-look permeability estimates using sidewall samples and porosity logs. 6th annual European logging symposium transactions, 1979.

VAN DER BAAN, M. and JUTTEN, C., 2000. Neural networks in geophysical applications. Geophysics, 65 (4). pp. 1032-1047. ISSN 0016-8033

VAPNIK, V.N., 1999. An overview of statistical learning theory. IEEE Transactions on Neural Networks, 10(5), pp. 988-999.

WALKER, E. & GLOVER, P.W.J., Characteristic pore size, permeability and the electrokinetic coupling coefficient transition frequency in porous media, Geophysics, 75(6), E235-E246, 2010.

WALKER, E. and GLOVER, P.W.J., 2018. Measurements of the Relationship Between Microstructure, pH, and the Streaming and Zeta Potentials of Sandstones. Transport in Porous Media, 121(1), pp. 183-206.

WANG, H., WU, W., CHEN, T., DONG, X. and WANG, G., 2019. An improved neural network for TOC, S1 and S2 estimation based on conventional well logs. Journal of Petroleum Science and Engineering, 176, pp. 664-678.

XUE, Y., CHENG, L., MOU, J. and ZHAO, W., 2014. A new fracture prediction method by combining genetic algorithm with neural network in low-permeability reservoirs. Journal of Petroleum Science and Engineering, 121, pp. 159-166.

YARVEICY, H. and GHIASI, M.M., 2017. Modeling of gas hydrate phase equilibria: Extremely randomized trees and LSSVM approaches. Journal of Molecular Liquids, 243, pp. 533-541.

YARVEICY, H., GHIASI, M.M. and MOHAMMADI, A.H., 2018. Performance evaluation of the machine learning approaches in modeling of CO2 equilibrium absorption in Piperazine aqueous solution. Journal of Molecular Liquids, 255, pp. 375-383.

YARVEICY, H., MOGHADDAM, A.K. and GHIASI, M.M., 2014. Practical use of statistical learning theory for modeling freezing point depression of electrolyte solutions: LSSVM model. Journal of Natural Gas Science and Engineering, 20, pp. 414-421.

ZHANG, X., SPIERS, C. J., PEACH, C. J., & HEBING, A. 2013. Tight rock permeability measurement by pressure pulse decay and modeling. Int. Symp. Soc. Core Anal., Napa Valley, California, USA, 16-19 September, 2013, 12 pp, SCA2013-10.

ZHOU, X., ZHANG, C., ZHANG, Z., ZHANG, R., ZHU, L., ZHANG, C., 2019. A saturation evaluation method in tight gas sandstones based on diagenetic facies. Marine and Petroleum Geology 107 (2019) 310–325.

ZHU, L., ZHANG, C., WEI, Y., ZHANG, C. 2017a. Permeability prediction of the tight sandstone reservoirs using hybrid intelligent algorithm and nuclear magnetic resonance logging data. Arab J. Sci. Eng. 42:1643–1654, DOI 10.1007/s13369-016-2365-2

ZHU, L., ZHANG, C., WEI, Y., ZHOU, X., HUANG, Y., and ZHANG, C., 2017b. Inversion of the permeability of a tight gas reservoir with the combination of a deep Boltzmann kernel extreme learning machine and nuclear magnetic resonance logging transverse relaxation time spectrum data. Interpretation 5: T341-T350. https://doi.org/10.1190/INT-2016-0188.1

ZHU, L., ZHANG, C., ZHANG, C., WEI, Y., ZHOU, X., CHENG, Y., HUANG, Y. and ZHANG, L., 2018, Prediction of total organic carbon content in shale reservoir based on a new integrated hybrid neural network and conventional well logging curves, J. Geophys. Eng., 15, 1050–1061, https://doi.org/10.1088/1742-2140/aaa7af

ZHU, L., ZHANG, C., ZHANG, C., ZHANG, Z., NIE, X., ZHOU, X., LIU, W., WANG, X., 2019a. Forming a new small sample deep learning model to predict total organic carbon content by combining unsupervised learning with semi-supervised learning, Applied Soft Computing Journal, 83, 105596, 10.1016/j.asoc.2019.105596

ZHU, L., ZHANG, C., ZHANG, C., ZHANG, Z., ZHOU, X., ZHU, B., 2019b. An improved theoretical nonelectric water saturation method for organic shale reservoirs, IEEEAccess, 7, 2169-3536, 10.1109/ACCESS.2019.2912214